ESTIMATING AN UAV OPERATOR'S COGNITIVE WORKLOAD BY MEASURING PUPIL DILATION

Konstantin Metodiev

Space Research and Technology Institute – Bulgarian Academy of Sciences
e-mail: komet@space.bas.bg

Keywords: *eye tracker, UAV, cognitive workload, wavelet*

Abstract: *In the paper hereby, results obtained after measuring an UAV operator's cognitive workload are announced. Simulation studies have been carried out on RC flight simulator including a genuine control radio in the loop. Throughout course of the flight session, pupil dilation is being measured simultaneously by means of a desktop-based eye tracker. The obtained signal is processed further by discrete wavelet transformation in order to split up both abrupt and gradual changes of pupil diameter. The former pattern supposedly comes as a consequence of cognitive effort whilst the latter should be attributed to ambient light conditions. Blinks have been taken into account and excluded from the stage of postprocessing results.*

Cognitive workload is presented with regard to number of abrupt oscillations of pupil diameter. Results have been obtained by means of developing source code in GNU Octave.

ОПРЕДЕЛЯНЕ НА КОГНИТИВНОТО НАТОВАРВАНЕ НА ОПЕРАТОР НА БЛА ЧРЕЗ ИЗМЕРВАНЕ РАЗШИРЕНИЕТО НА ЗЕНИЦАТА

Константин Методиев

Институт за космически изследвания и технологии – Българска академия на науките
e-mail: komet@space.bas.bg

Ключови думи: *окулограф, БЛА, когнитивно натоварване, уейвлет функция*

Резюме: *В настоящия доклад са представени резултати, получени след измерване когнитивното натоварване на оператор на БЛА. Проведени са полунатурни изследвания на симулатор, включващ реална апаратура за управление. По време на експеримента диаметърът на зеницата се измерва чрез настолен окулограф в реално време. Полученият сигнал се обработва чрез дискретна уейвлет трансформация, за да се разделят резки и монотонни изменения в диаметъра на зеницата. За първия модел на изменение се предполага, че се дължи на когнитивно натоварване, а за втория – на осветеността на работната среда. Премигванията са отчетени и изключени от етапа на обработка на резултатите.*

Когнитивното натоварване е определено в зависимост от броя на резките осцилацци на диаметъра на зеницата. Резултатите са получени посредством разработка на код на GNU Octave.

Introduction

Task of measuring pupil dilation comes down to setting apart two reflexes of the visual analyzer muscles, which often occur simultaneously. Two muscle groups control the pupil dilation: the circular muscles surrounding the pupil and the radial muscles extending from the pupil to the iris periphery. Under the influence of a light stimulus, the circular muscles are activated and the radial ones are suppressed, thus causing the pupil to contract. On the contrary, under the influence of a cognitive stimulus, the radial muscles are activated and the circular ones are inhibited, which provokes an abrupt dilation of the pupil diameter.

The study hereby aims at identifying events of high cognitive workload during flight task performed on RC flight simulator. The research methodology has adopted to some extent what is described in patent [1] by Sandra P. Marshall. All credits are due to the respectful inventor.

Materials and Methods

The experiment setup consists of a PC, Gazepoint GP3 HD eye tracker, [2], Taranis X9D+ radio transmitter, [3], RC to USB KSim dongle, Phoenix RC 6.0.i RC flight simulator, [4], and a RC helicopter, Fig. 1. A trainee is told to perform take off, basic flight manoeuvres, and land within two minutes. During flight session, the eye tracker is gathering data about pupil diameter variations and blinks at sampling rate of 150 Hz. The ambient light conditions are set constant.

Fig. 1. Experiment setup: Thunder Tiger Raptor 90 G4 put on the screen

The undecimated discrete wavelet transformation (UDWT) has been chosen to separate frequency components of the pupil diameter signal. A flowchart depicting two-level implementation is shown in Fig. 2. It comprises two nested single-level UDWTs. Two stages are recognizably different during transformation, i.e. decomposition and reconstruction stage, hence the indices **d** and **r**. During decomposition stage, the input signal **S** is being passed to high pass (**Hid**) and low pass (**Lod**) filters to carry out discrete convolution. After filtering, low (**cA**, approximations) and high (**cD**, details) frequency components are split up. The signal of approximation coefficients **cA** closely resembles the input one. The signal of detail coefficients **cD** is less informative, though it is of particular interest in the present study.

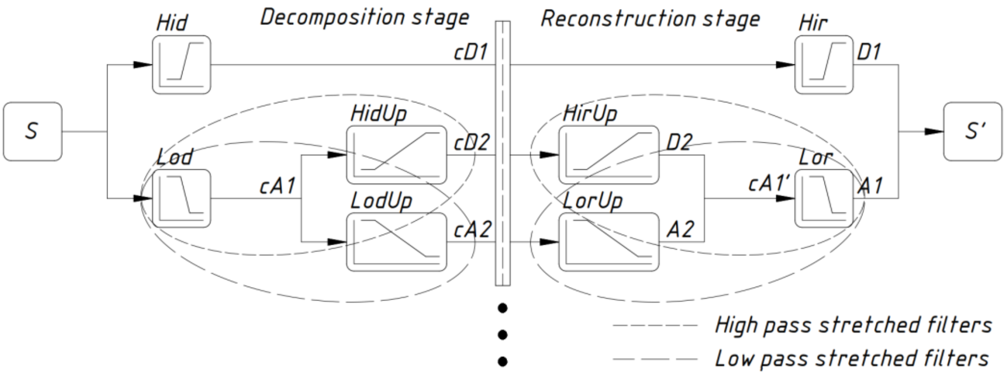

Fig. 2. Two-level undecimated discrete wavelet transformation flowchart

An arbitrary level of transformation might be chosen in order to achieve desired level of signal denoising or compression. The cascaded multilevel signal decomposition / reconstruction is widely known as Mallat's algorithm, [5]. In case of undecimated implementation, filters are stretched at each level to narrow the frequency pass band and decrease the center frequency while the peak value doubles (**Q** behavior), [6].

In present study, Daubeches **Db2** wavelet has been chosen. Low order (of two) makes it feasible for the wavelet to extract high frequencies obtainable from the input signal. Four basic filters associated with **Db2** wavelet are shown in Table 1.

Table 1. Basic **Db2** filters

Hir = [-0.1294, -0.2241, 0.8365, -0.4830];	**basic**
Hid = [-0.4830, 0.8365, -0.2241, -0.1294];	
Lod = [-0.1294, 0.2241, 0.8365, 0.4830];	
Lor = [0.4830, 0.8365, 0.2241, -0.1294];	**scaling**

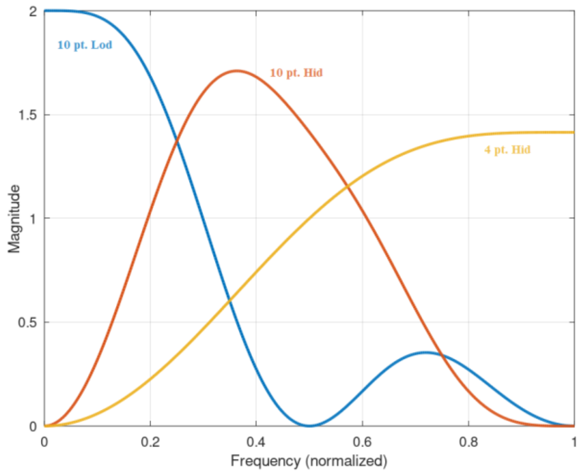

Fig. 3. Db2 filterbank used in case of two-level UDWT (frequency responses)

Filter stretching is performed by upsamplig dyadically basic **Db2** filters (Table 1) and convolving by low pass filter at preceding level of transformation. In Fig. 2, filters falling within each dashed oval line illustrate the idea. Frequency responses, Fig. 3, of both basic and stretched filters used at decomposition stage, in case of two-level UDWT, might be depicted in GNU Octave environment, [7], by means of following script. LtFat library, [8], [9], is required.

```
[g, a] = wfbt2filterbank({'db2',2,'dwt'});
filterbankfreqz(g,a,1024,'plot','linabs','posfreq');
```

Alternatively, frequency and phase responses of stretched filters might be acquired by running the script below. In this particular example, high pass decomposition filter has been taken into consideration, Table 1. The prerequisite is Signal library.

```
db2 = Hir; filter = Lor;
db2 = upsample(db2, 2); db2(end) = [];
db2 = conv(db2, filter);
[h, w] = freqz(db2);
figure(1); plot(w/pi, abs(h));
figure(2); plot(w/pi, unwrap(arg(h), pi) / pi);
```

Non-linear phase response of both basic and stretched filters introduces –kπ rad worth of lag at Nyquist (folding) frequency.

Increased cognitive workload dilates pupil diameter rapidly. The phenomenon is called Dilation Reflex. It is a transitory event. Abrupt changes of pupil diameter are considered irregular and sharp consisting of large jumps followed by rapid declines, [1]. Therefore, these changes are to be looked for in the detail coefficient **cD1** signal. Pupil light reflex is thought to be filtered out and solely observable in the approximation coefficient **cA2** signal.

The high frequency signal **cD1** is believed to have been corrupted by noise. In paper [10], authors come up with algorithms of signal thresholding. All decomposed coefficients smaller than expected maximum are zeroed. Noise is assumed normally distributed. The universal threshold method, based on noise standard deviation $\boldsymbol{\sigma}$, [10], is computed according to formula

(1) $$\lambda^U = \sigma\sqrt{2\ln(N)}$$

where N is the sample size. In most cases $\boldsymbol{\sigma}$ is unknown, though it might be estimated by

(2) $$\sigma \approx \frac{median(|x_i|)}{0.67449}$$

where $\mathbf{x_i}$ is ith sample. One way of threshold utilizing is the so-called Hard Thresholding Method

(3) $$x_i = \begin{cases} 0 & if\ |x_i| \le \lambda^U \\ x_i & if\ |x_i| > \lambda^U \end{cases}$$

which is also available in LtFat library

```
[xi, N] = thresh(xi,lambda,'hard');
```

Time – Frequency Localization

The proposed algorithm has been put to the test by means of two exact signals with frequency components of $\mathbf{f_1}$ = 10 Hz and $\mathbf{f_2}$ = 100 Hz. The sampling frequency $\mathbf{f_s}$ was set 4 times the highest signal frequency. The former signal is periodic containing two superposed cosine functions whilst the latter assumes a definite form of split cosine function. The wave equations are following:

$$x_1 = \cos\left(2\pi f_1 t\right) + \cos\left(2\pi f_2 t\right) \quad t \in \left[0;1\right]$$

(4)

$$x_2 = \begin{cases} \cos\left(2\pi f_1 t\right) & t \in \left[0;1\right] \\ \cos\left(2\pi f_2 t\right) & t \in \left(1;2\right] \end{cases}$$

Both signals might be seen in Fig. 4 alongside power spectra obtained by means of Fast Fourier Transformation (FFT). Although set, this problem clearly reveals inability of FFT to discriminate frequency components over time for both spectra are virtually identical. In this case, the FFT is said to be localized poorly in time.

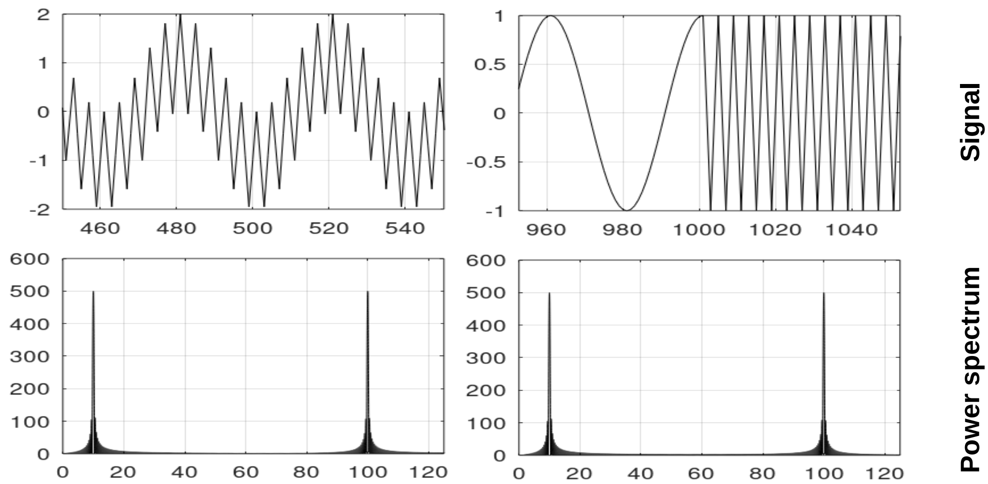

Fig. 4. FFT applied to both periodic (left) and split cosine signals

Two-level Undecimated Discrete Wavelet Transformation was subsequently applied to both signals by requesting following function from the LtFat library:

```
[c, info] = ufwt(input,'db2',2,'noscale');
```

In Details and Approximations coefficients charts, Fig. 5, the frequency components are distinctly set apart on account of a good time – frequency localization of wavelet transformation. Wavelets are known to have a limited time-interval as well as a limited bandwidth, [6].

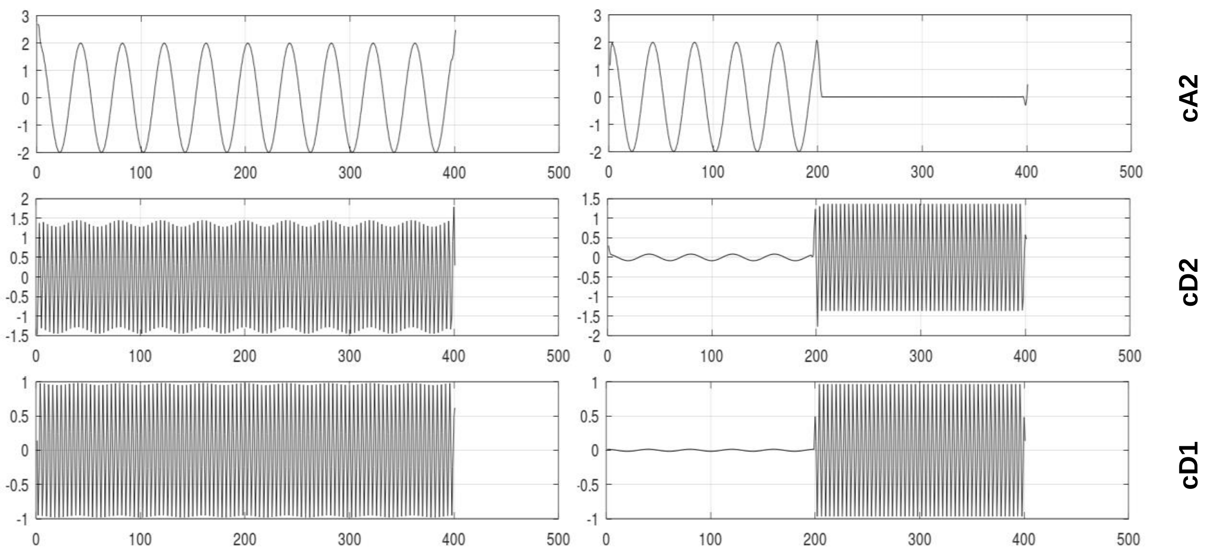

Fig. 5. Two-level UDWT applied to both periodic (left) and split cosine signal

Results

Details and approximations coefficients, obtained after applying two-level UDWT, for left pupil, are shown in Fig. 6 as well as raw data sets.

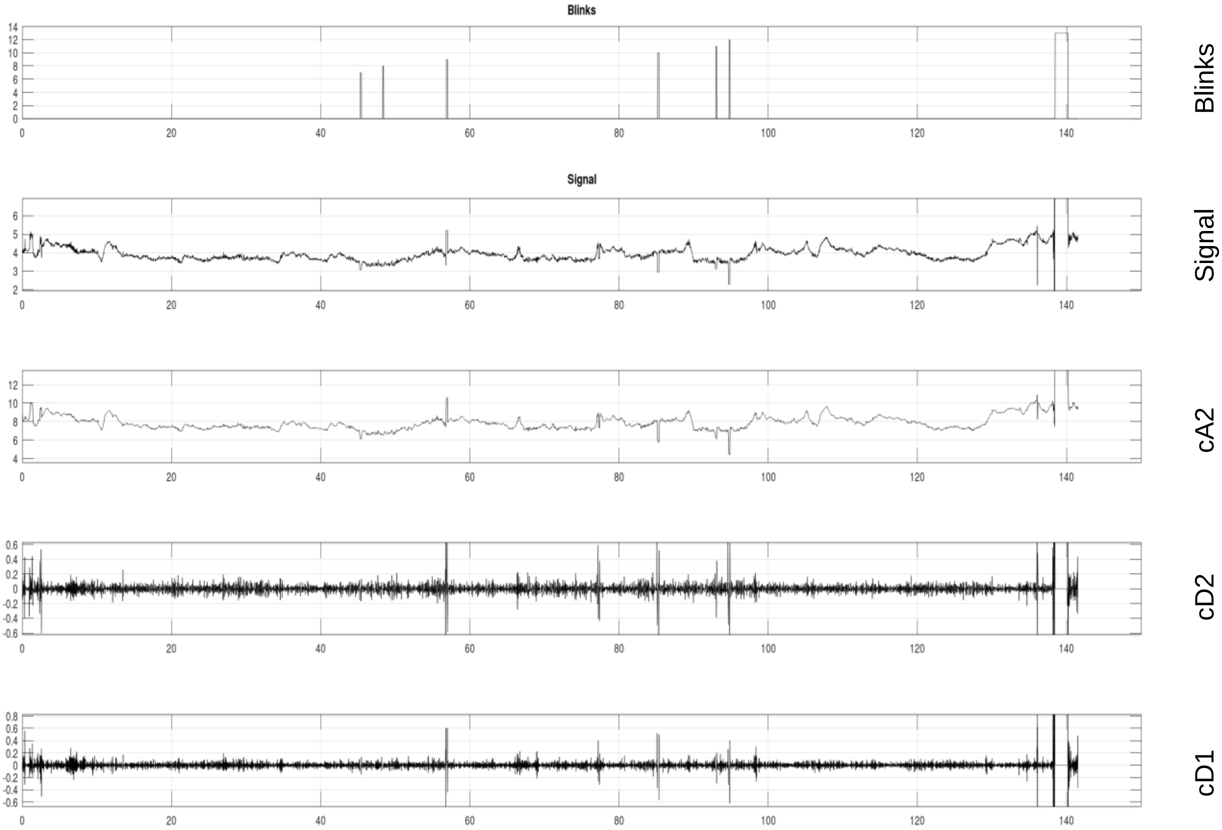

Fig. 6. Raw data and decomposed signal, left pupil

In addition, in following Fig. 7, denoised **cD1** coefficients, computed according to formulae (1) … (3) are shown alongside recorded blinks.

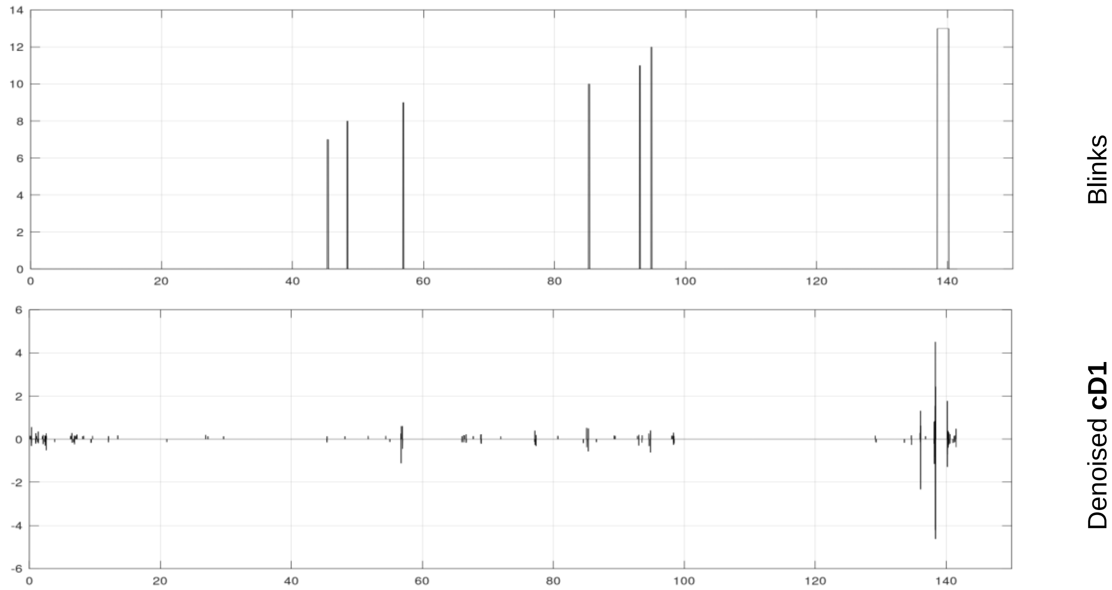

Fig. 7. Denoised **cD1** coefficients

The computed threshold level is $\lambda^U = 0.1289$. The hard thresholding method preserved 161 samples out of 8584 in total. Sample onsets coinciding with blinks (7 in total) are to be neglected. Remaining samples are identified as events during which the cognitive load has risen. In order to localize these events, one may look up in the video stream.

Discourse

A binary vector might be defined subsequently within limited interval of interest. The vector length depends upon the eye tracker sampling frequency. Gazepoint GP3 HD eye tracker gathers data at rate of 150 Hz. Therefore, the vector is `floor(150 times seconds)` elements long. An expected time period between two consecutive samples is 6.7 ms. Whenever non-zero samples are encountered in denoised **cD1** signal, the vector takes non-zero elements. In this way, the vector might indicate a noticeably different pupil activity, [1], attributed to increasing cognitive workload.

Choice of basic wavelet number of coefficients (i.e. order) appears to be essential. Daubeches wavelets are suitable for solving signal self-similarity properties at separate scales as well as signal discontinuities. To extract information from the signal is based on number of zero moments equal to half the number of wavelet coefficients. The higher number of the zero moments, the better ability of wavelet to delineate a polynomial behaviour of the input signal. It is highly up to an experienced researcher to make a definitive decision. In addition, decomposition might be repeated to keep on dividing frequency band to sub-bands (further increase frequency resolution of the coefficient signal). Last but not the least, the obtained results might be enhanced by EEG measurements carried out simultaneously.

Acknowledgements

The Bulgarian National Science Fund at the Republic of Bulgaria has been supporting the research hereby since 11th of December, 2018, according to contract № КП-06/Н27-10. The project title is “Human Factor in Remotely Controlled Aerial Systems – Analysis, Estimation, and Control.”

References:

1. Marshall, Sandra P., Method and Apparatus for Eye Tracking and Monitoring Pupil Dilation to Evaluate Cognitive Activity, patent US006090051A, 18th of July, 2000
2. https://www.gazept.com
3. https://www.frsky-rc.com/
4. https://www.rc-thoughts.com/phoenix-sim/
5. Mallat, S. G. “A Theory for Multiresolution Signal Decomposition: The Wavelet Representation,” IEEE Transactions on Pattern Analysis and Machine Intelligence. Vol. 11, Issue 7, July 1989, pp. 674–693.
6. Fugal, D. Lee, Conceptual Wavelets in Digital Signal Processing, an In-Depth Practical Approach for the Non-Mathematician, Space & Signals Technical Publishing, San Diego, California, 2009, p.p. 120, 134 http://www.conceptualwavelets.com/, ISBN: 978-0-9821994-5-9
7. Eaton, John W., David Bateman, Søren Hauberg, Rik Wehbring (2020). GNU Octave version 6.1.0 manual: a high-level interactive language for numerical computations. https://www.gnu.org/software/octave/doc/v6.1.0/
8. Průša, Zdeněk, Peter L. Søndergaard, Nicki Holighaus, Christoph Wiesmeyr, Peter Balazs, The Large Time-Frequency Analysis Toolbox 2.0. Sound, Music, and Motion, Lecture Notes in Computer Science 2014, pp 419–442
9. Søndergaard, Peter L., Bruno Torrésani, Peter Balazs. The Linear Time-Frequency Analysis Toolbox. International Journal of Wavelets, Multiresolution Analysis and Information Processing, 10(4), 2012
10. Donoho, D. L., in Proceedings of Symposia in Applied Mathematics: Different Perspectives on Wavelets; Daubechies, I., Ed.; American Mathematical Society: Providence, RI, 1993; Nonlinear Wavelet Methods for Recovery of Signals, Densities, and Spectra from Indirect and Noisy Data pp 173–205